Supporting Information

CeO_6Te_2 Nanosheets for Multifunctional Broadband Visible Light Photo Detection and NLO Applications: An Experimental & Computational Approach

Prabhukrupa Chinmay Kumar[1], Soumya Pattnaik[1], Jagadish Kumar[2,3], Chinnaiyah Sripan[4], Jnanranjan Panda[5], Ramakanta Naik[1]*

[1] *Department of Engineering and Materials Physics, Institute of Chemical Technology-Indian Oil Odisha Campus, Bhubaneswar, 751013, India*

[2] *Department of Physics and Astrophysics, University of Delhi, Delhi-110007, India*

[3] *Department of Physics, Centre for High Energy and Condensed Matter Physics, Utkal University, Vani Vihar, Bhubaneswar 751004, India*

[4] *Department of Physics, Dayananda Sagar Academy of Technology and Management, Udayapura, Bangalore, 560082, India*

[5] *Faculty of Science, Sri Sri University, Cuttack-754006, India*

[*] *Corresponding author:* ramakanta.naik@gmail.com

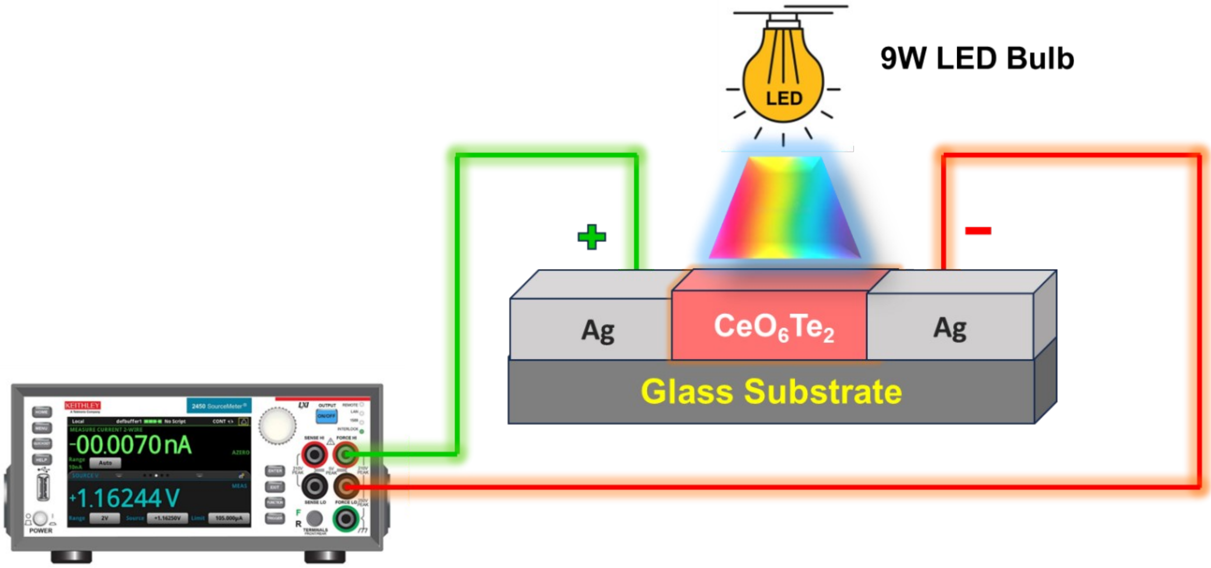

Scheme S1. Exhibiting the photo response measurement setup.

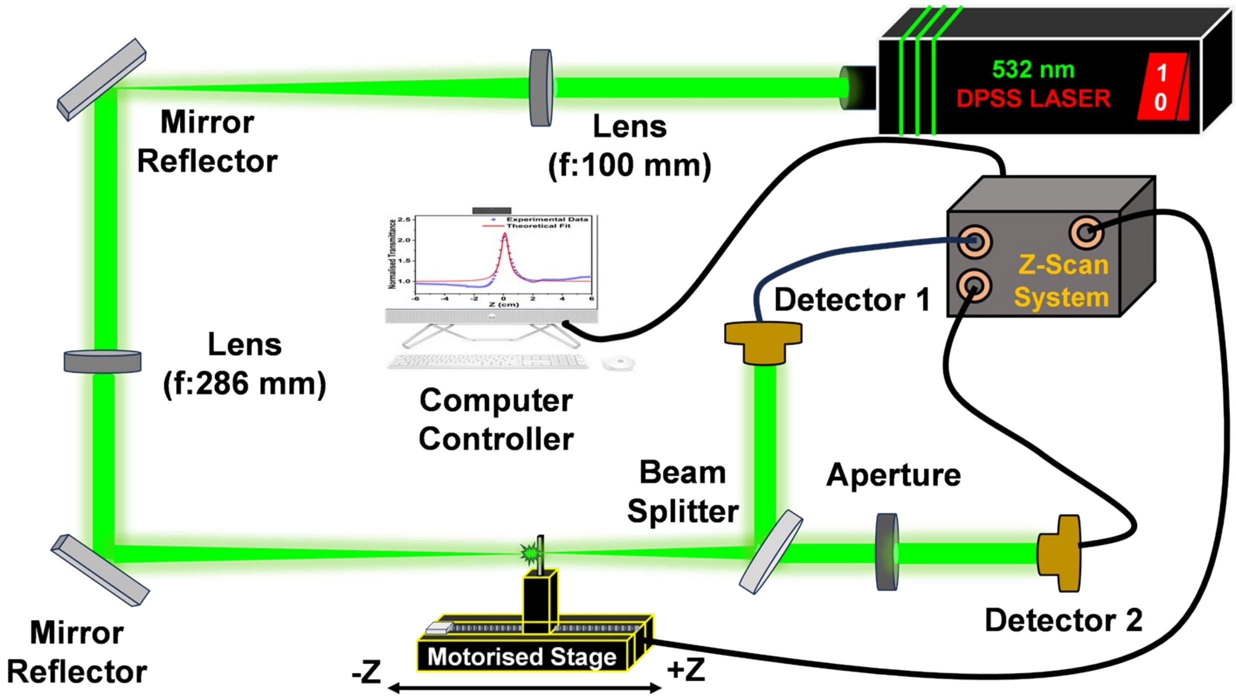

Scheme S2. Demonstrating the Z-scan measurement setup with all the components used in the process.

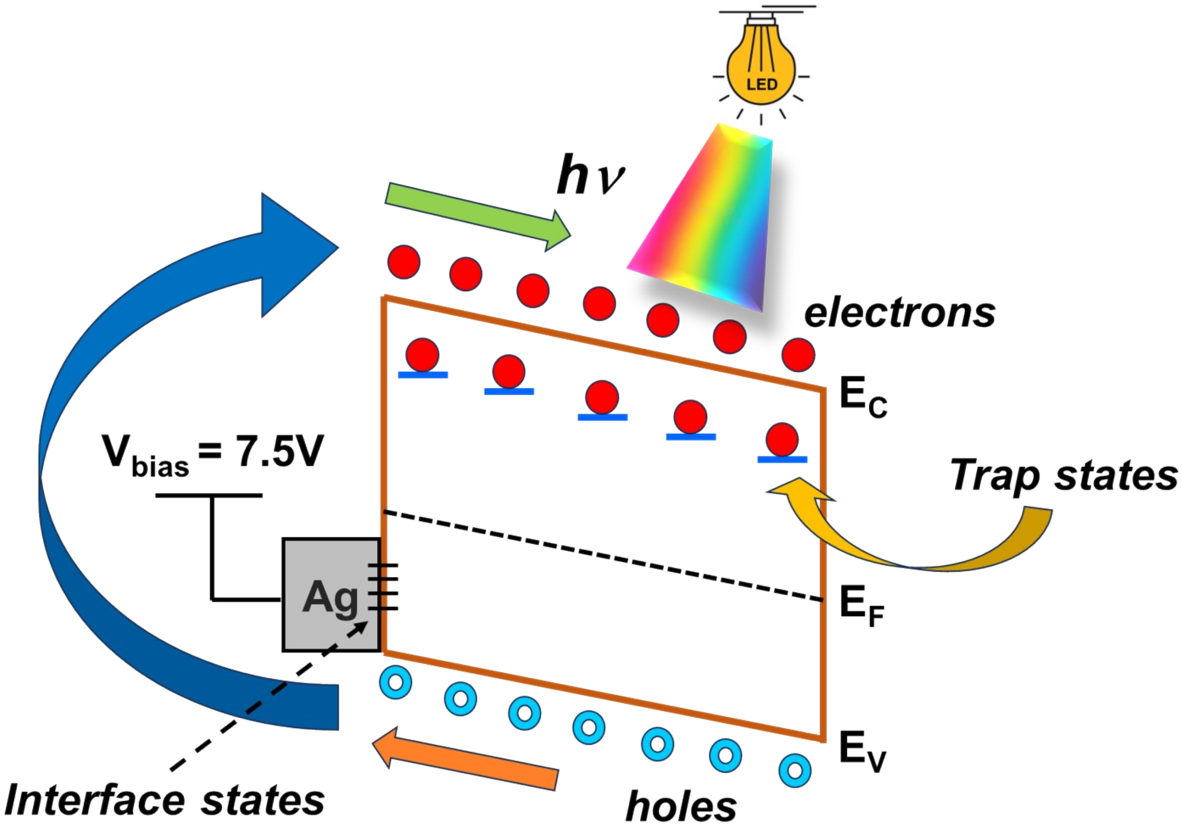

Scheme S3. Schematic representation of band diagram of the device depicting the charge transport and recombination mechanisms of the COT PDs during photodetection process.

Table S1. Structural parameters obtained from XRD peak analysis.

Samples	Average Crystallite Size (D) (nm)	Dislocation density(δ) $\times 10^{-3}$ (nm^2)	Lattice Strain (ε) $\times 10^{-3}$
COT-1	89.12	5.97	9.65
COT-2	52.24	3.61	5.18
COT-3	73.49	5.07	1.25

Table S2. Elemental Ce, O, and Te atomic percentages for different COT NS.

Sample	COT-1	COT-2	COT-3
Element	At. %	At. %	At. %
Ce	27.45	29.83	31.90
O	45.01	42.37	41.70
Te	27.54	27.80	26.40
Total	100.00	100.00	100.00

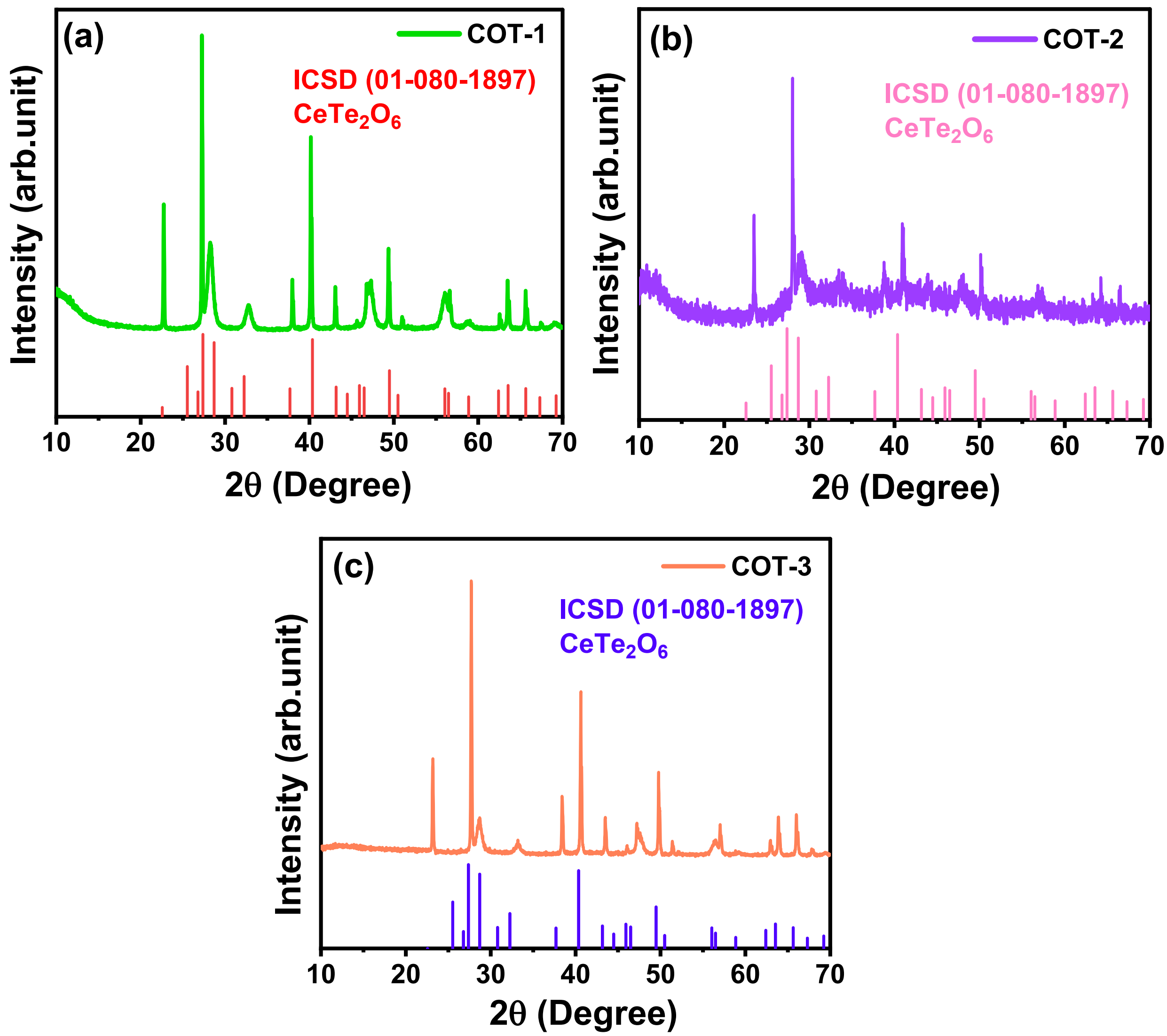

Fig. S1. XRD patterns of each sample (a) COT-1, (b) COT-2, and (c) COT-3 matched against the respective ICSD cards.

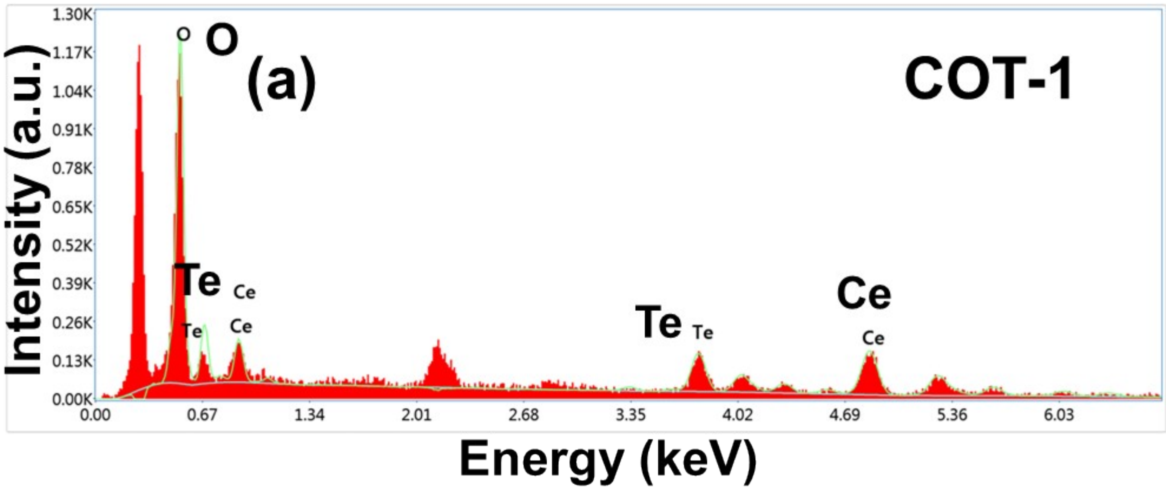

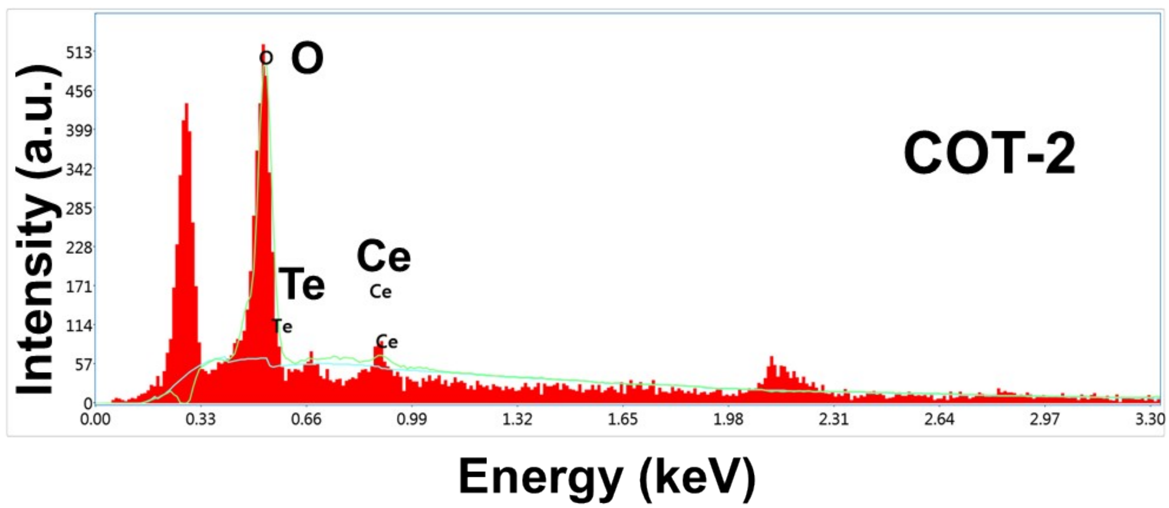

Fig. S2. EDX spectra of (a) COT-1, and (b) COT-2 samples.

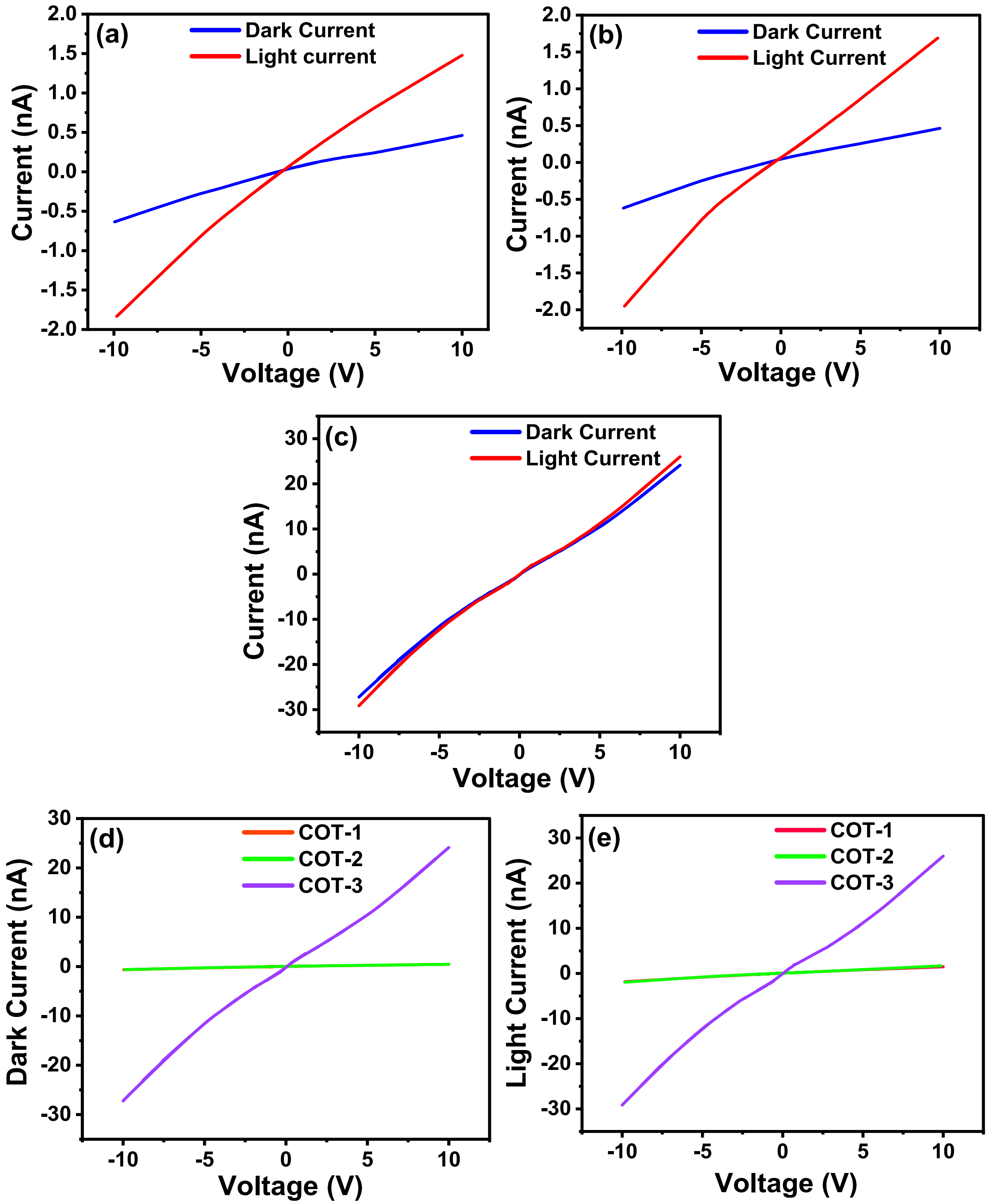

Fig. S3. I ~V characteristic plots with the linear y-axis of individual samples (a) COT-1, (b) COT-2, (c) COT-3, combined plots of all samples under (d) dark and (e) light states respectively.

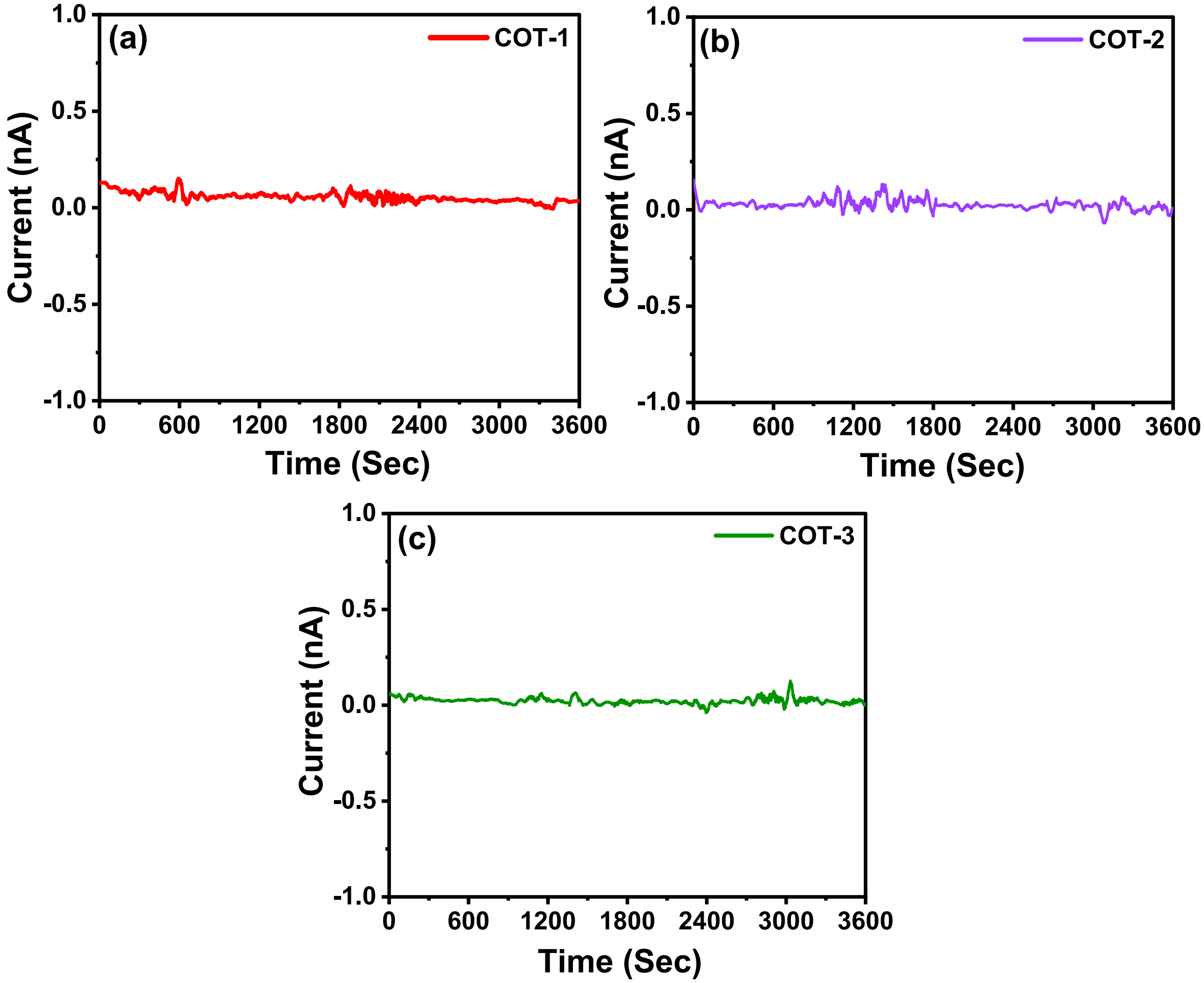

Fig. S4. I~T stability plots of (a) COT-1, (b) COT-2, (c) COT-3 samples, respectively.

Table S3. Comparison of photo detector parameters of different metal oxychalcogenide materials.

Photodetector materials	Wavelength (nm)	Responsivity (R) (AW^{-1})	Detectivity (D*) (Jones)	Refs.
Bi_2O_2S	850	9.48×10^{-3}	9.96×10^{10}	1
Bi_2O_2Se	300-900	3.712×10^{3}	3.3×10^{10}	2
Bi_2O_2Te	210-2400	3×10^{5}	4×10^{15}	3
Bi_2O_5Te	400-700 (Vis)	1.55×10^{-4}	2.18×10^{12}	4
La_2O_6Te	400-700 (Vis)	10.64×10^{-6}	5.8×10^{7}	5
$V_2O_9Te_2$	400-700 (Vis)	5.35×10^{-6}	3.45×10^{7}	6
CeO_6Te_2	400-700 (Vis)	5.20×10^{-6}	2.95×10^{7}	This work

Table S4. NLO parameters of different materials are underperformed in CW laser mode.

Sample Name	β (cm/W)	n_2 (cm^2 / W)	$\chi^{(3)}$ (e.s.u.)	References
N-GO	0.14×10^{-6}	5.75×10^{-13}	3.25×10^{-7}	7
GO rGO	2.1×10^{-6} 9×10^{-6}	1.0203×10^{-11} 9.5549×10^{-11}	_	8
CDs	2.513×10^{-4}	1.012×10^{-8}	3.93×10^{-7}	9
THBSM crystal	2.014×10^{-3}	2.324×10^{-7}	7.504×10^{-5}	10
CdTe	1.4×10^{-2}	2.58×10^{-7}	_	11
La_2O_6Te	3.798×10^{-3}	3.592×10^{-8}	5.826×10^{-3}	5
VS_2 /MoS_2	0.139×10^{-5}	1.758×10^{-5}	_	12
$V_2O_9Te_2$	8.08×10^{-3}	3.515×10^{-8}	4.263×10^{-3}	6
CeO_6Te_2	69.2×10^{-3}	25.755×10^{-8}	62.586×10^{-3}	This work

Reference:

[1] P. Rong, S. Gao, M. Zhang, S. Ren, H. Lu, J. Jia, S. Jiao, Y. Zhang and J. Wang, Large-area hierarchical Bi_2O_2S flowers composed of 2D ultrathin nanosheets for high performance self-powered IR photodetector, *J. Alloys Compd.*, 2022, **928**, 167128.

[2] X. Zou, R. Wang, Y. Sun and C. Wang, Two-dimensional Bi_2O_2Se nanosheets for sensitive and fast-response high-temperature photodetectors, *J. Materiomics*, 2023, **9**, 10241031.

[3] P. Tian, H. Wu, L. Tang, J. Xiang, R. Ji, S. P. Lau, K. S. Teng, W. Guo, Y. Yao and L.-J. Li, Ultrasensitive broadband photodetectors based on two-dimensional Bi_2O_2Te films, *J. Mater. Chem. C*, 2021, **9**, 13713–13721.

[4] P.C. Kumar, G.K. Pradhan, S. Senapati, R. Naik, Two-dimensional Bi_2O_5Te nanosheets for sensitive and fast response broadband visible light photodetectors, *ACS Appl. Electron. Mater.*, 2024, **6**, 3311-3324.

[5] P.C. Kumar, S. Supriya, A. Mohapatra, S. Chinnaiyah, R. Naik, Enhanced two-photon absorption in hydrothermally synthesized La_2O_6Te nanorods for visible light photodetection, Nanoscale, 2025, **17**, 2326-2344.

[6] Kumar, P.C., Kumar, J., Sripan, C. and Naik, R., $V_2O_9Te_2$ Nanorods for broadband visible light photoresponse and NLO applications: An experimental and computational approach, *ACS Appl. Electron. Mater.* 2025, **7**, 5842–5860.

[7] K. Kumara, T. C. S. Shetty, S. R. Maidur, P. S. Patil and S. M. Dharmaprakash, Continuous wave laser induced nonlinear optical response of nitrogen doped graphene oxide, *Optik*, 2019, **178**, 384-393.

[8] K. Kumara, V. S. Kindalkar, F. J. Serrao, T. C. S. Shetty, P.S. Patil and S.M. Dharmaprakash, Enhanced nonlinear optical absorption in defect enriched graphene oxide and reduced graphene oxide using continuous wave laser z-scan technique *Mater. Today Proc.*, 2022, **55**, 186-193.

[9] S. Pandiyan, L. Arumugam, S. P. Srirengan, R. Pitchan, P. Sevugan, K. Kannan, G. Pitchan, T. A. Hegde and V. Gandhirajan, Biocompatible Carbon Quantum Dots Derived from Sugarcane

Industrial Wastes for Effective Nonlinear Optical Behavior and Antimicrobial Activity Applications, *ACS omega*, 2020, **5**, 30363-30372.

[10] A. Priyadharshini and S. Kalainathan, Synthesis, structure and characterization of new promising organic NLO crystal: thiosemicarbazide 4-hydroxybenzenesulfonate monohydrate (THBSM), *J Mater Sci: Mater Electron*, 2017, **28**,7401–7412.

[11] M. H. Majles Ara, Z. Moslemi, H. Naderi, A. Mihandoost, A. Daneshfar and R. Sahraei, Nonlinear optical properties of CdTe nanocrystals synthesized by a green room temperature solution method, *Applied Physics B*, 2015, **118**, 567-572.

[12] B. Dandasena, S. Das, Prabhukrupa C. Kumar, S. Supriya, R. Naik; VS_2/MoS_2 nanocomposite with reverse saturable absorption for optical limiting and nonlinear optical applications. J. Appl. Phys., 2025, **137**, 043101.